

# Surface Behavior of Boronic Acid-Terminated Silicones

*Erum Mansuri<sup>a</sup>, Laura Zepeda-Velazquez<sup>b</sup>, Rolf Schmidt<sup>a</sup>, Michael A. Brook<sup>b,\*</sup>, Christine E.  
DeWolf<sup>a,\*</sup>*

<sup>a</sup>Department of Chemistry and Biochemistry and Concordia Centre for NanoScience Research,  
Concordia University, 7141 Sherbrooke St. W., Montréal, Québec, Canada H4B 1R6

<sup>b</sup>Department of Chemistry and Chemical Biology, McMaster University, 1280 Main St. W.,  
Hamilton, Ontario, Canada L8S 4M1

## Supporting Information

### Brewster angle microscopy

Brewster angle microscopy is used to follow film morphology changes throughout the compression isotherms; images obtained for functionalized and non-functionalized PDMS at the air-water interface are shown in Figure S1. At very low pressures a two-dimensional foam can be observed as has previously been reported.<sup>1,2</sup> Beyond the critical area at which pressure begins to increase, no contrast can be observed within the films, even across most of the plateau region. For both end-functionalized and non-functionalized PDMS, small, very bright domains are observed starting at mid-way through the plateau region, although it should be noted that the density of domains is not uniform across the film, i.e. there are regions of a high and low density

of domains. The formation of such domains for PDMS has been previously reported in literature, and are associated autophobic dewetting of PDMS.<sup>1,3-5</sup> From the BAM images, it can be seen that these domains grow in density and brightness as the film is compressed, the latter indicating that they are much thicker than the rest of the film. Both the functionalized and non-functionalized films display similar morphologies despite the differences in the isotherms and in ellipsometry in this region.

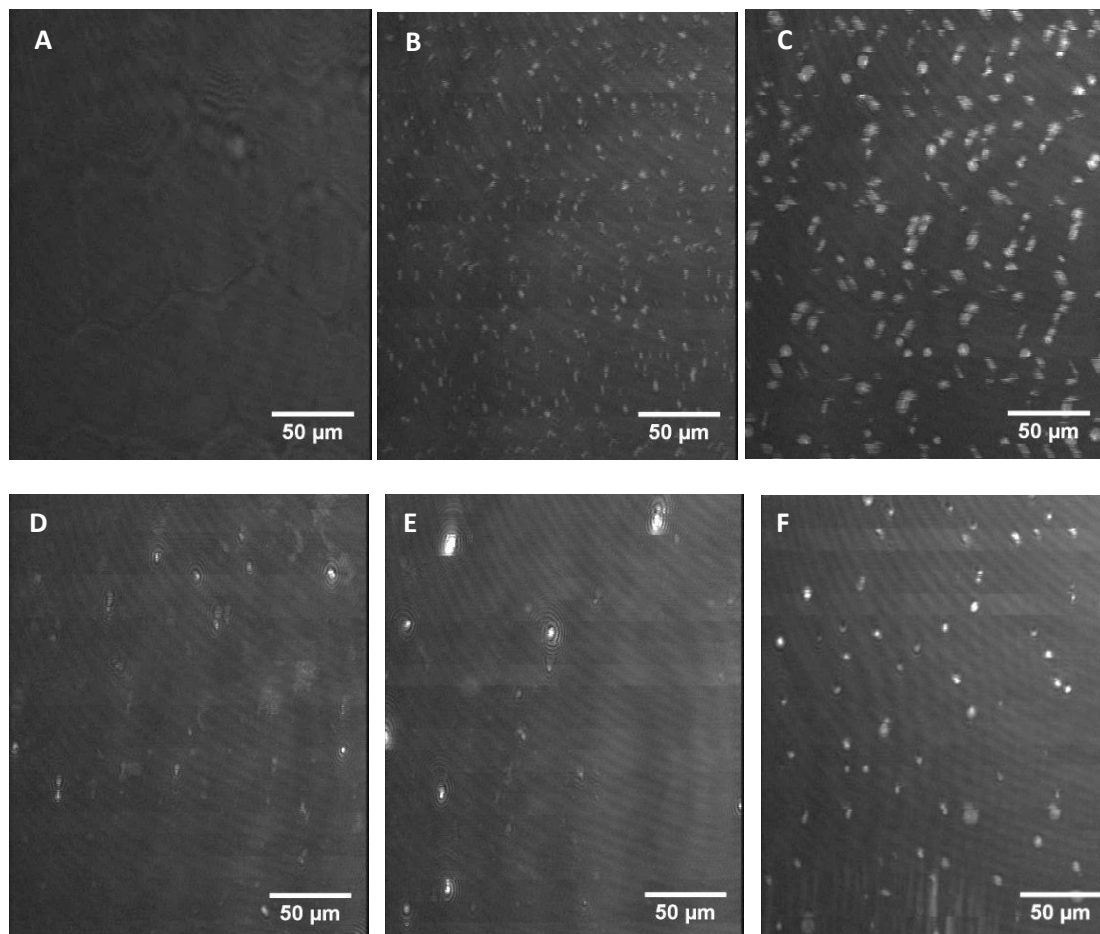


Figure S1. *Top row* (images A-C), BAM images for SiBA-10 (A:  $246 \text{ \AA}^2 \cdot \text{molecule}^{-1}$ ,  $0.2 \text{ mN} \cdot \text{m}^{-1}$ ; B:  $64 \text{ \AA}^2 \cdot \text{molecule}^{-1}$ ,  $23 \text{ mN} \cdot \text{m}^{-1}$ ; C:  $48 \text{ \AA}^2 \cdot \text{molecule}^{-1}$ ,  $26 \text{ mN} \cdot \text{m}^{-1}$ ). *Bottom row* (images D-F), BAM images for SiBA-69 (D:  $349 \text{ \AA}^2 \cdot \text{molecule}^{-1}$ ,  $11 \text{ mN} \cdot \text{m}^{-1}$ ; E:  $267 \text{ \AA}^2 \cdot \text{molecule}^{-1}$ ,  $12 \text{ mN} \cdot \text{m}^{-1}$ ) and H-PDMS-69 (F:  $377 \text{ \AA}^2 \cdot \text{molecule}^{-1}$ ,  $8 \text{ mN} \cdot \text{m}^{-1}$ ).

## Recompression isotherms

Figure S2 shows the recompression isotherms for SiBA-16. The overlapping expansion and subsequent recompression isotherms indicate that the hysteresis is generated by a slow respreading rather than a partial solubility of the SiBAs.

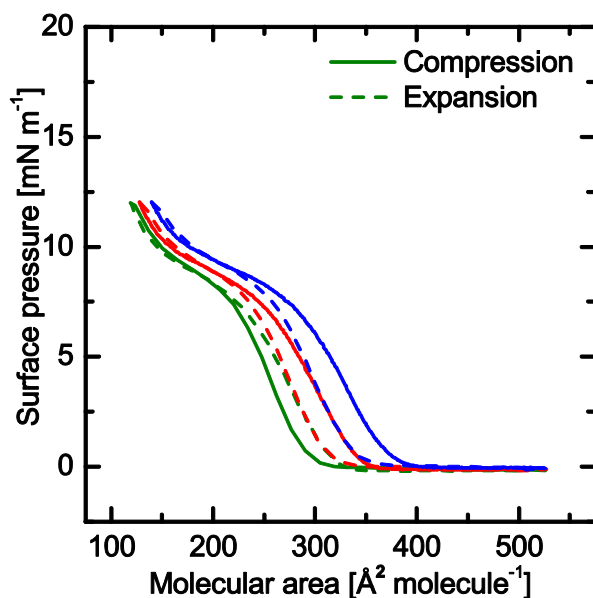


Figure S2. Isotherm for repeated compression-expansion cycles for SiBA-16 on water at room temperature where solid lines represent film compressions and dashed lines of the same color the corresponding film expansion. Recompression starts immediately after expansion without any equilibration time.

## References

- (1) Liao, Z.; Hsieh, W.-T.; Baumgart, T.; Dmochowski, I. J. *Langmuir* 2013, 29, 9420–9427.
- (2) Mann, E. K.; Henon, S.; Langevin, D.; Meunier, J. J. *Phys. II* 1992, 2, 1683–1704.

- (3) Mann, E. K.; Lee, L. T.; Henon, S.; Langevin, D.; Meunier, J. *Macromolecules* 1993, 26, 7037–7045.
- (4) Bernardini, C.; Stoyanov, S. D.; Cohen Stuart, M. A.; Arnaudov, L. N.; Leermakers, F. A. M. *Langmuir* 2010, 26, 11850–11861.
- (5) Reiter, G.; Sharma, A.; Casoli, A.; David, M.-O.; Khanna, R.; Auroy, P. *Langmuir* 1999, 15, 2551–2558.